

Doping effect of Al³⁺ on the structural and magnetic properties of Cobalt ferrite nanoparticles.

Vinod N. Dhage¹, Sopan M. Rathod^{1*}

¹Department of Physics, Abasaheb Garware College, Pune (M.S) INDIA – 411 004.

*smragc@rediffmail.com

ABSTRACT

The nanocrystalline aluminum substituted cobalt ferrite having general formula $\text{CoFe}_{2-x}\text{Al}_x\text{O}_4$ (where $x = 0.0, 0.2, 0.4, 0.6$) have been prepared by sol-gel auto combustion method. The precursors were prepared by using the stoichiometric amounts of Co^{2+} , Fe^{3+} and Al^{3+} nitrate solutions with citric acid as a chelating agent. The metal nitrate to citric acid ratio was taken as 1:2. The as prepared samples of aluminium substituted cobalt ferrite were sintered at 700°C for 5h. The Sintered samples of $\text{CoAl}_x\text{Fe}_{2-x}\text{O}_4$ system were characterized by XRD and VSM technique. The lattice constant obtained from XRD data decreases with increase in aluminum concentration x . The crystallite size obtained from X-ray diffraction is in 56-32 nm range which shows nanocrystalline nature of the prepared samples. The magnetic behaviour of the aluminum doped cobalt ferrite was studied by using room temperature vibrational sample magnetometry technique. The saturation magnetization (M_s), remanence magnetization (M_r) and Coercivity (H_c) was calculated by using hysteresis plots.

Keywords: nanocrystalline, chemical synthesis, X-ray diffraction, magnetic properties.

Corresponding author: Dr. Rathod S. M, Email Id: smragc@rediffmail.com

1. Introduction

Magnetic particles have become a subject of considerable interest in last few decades and many physical studies have been devoted to them. The ability to produce nanosized magnetic materials opened new application for magnetic materials such as magnetic data storage, magnetocaloric refrigeration, electronics, ferrofluid technology, magnetically targeted drug carriers, contrast agents in magnetic resonance imaging.

Nano-ferrites form an important class of magnetic materials because of their high resistivity and low energy losses (eddy current) and hence have vast technological application over wide range of frequencies [1]. Recent studies have shown that the physical properties of

nanoparticles are influenced significantly by the processing technique [2]. Since crystallite size, distribution of particle sizes and inter particle spacing have the greatest impact on magnetic properties. Many wet-chemical methods are employed for the preparation of the nano-sized spinel ferrite. One of them is sol-gel auto combustion which has recently become very popular technique. It is a simple process, which offers significant saving in time and energy consumption over the traditional methods and requires a low sintering temperature. This method is used to obtain improved properties, more homogeneity and narrow particle distribution thereby influencing structural, electrical and magnetic properties of spinel ferrite [3]. It is well known that, some magnetic properties such as saturation magnetization and coercivity depend strongly on the particle size and microstructure of the materials. Therefore, it is interesting and important to develop techniques by which the size and shape of the particles can be well controlled. One of the ways to prepare the nanocrystalline spinel ferrite material with required properties is Sol-gel auto combustion technique.

Among the spinel ferrite cobalt ferrite is well known ferrite with highly resistive properties. Cobalt ferrite belongs to a class of compounds having the general formula $M^{2+}Fe_2^{3+}O_4$ and crystallizing with inverse spinel structure [4]. The degree of inversion depends on the synthesis method and synthesis parameters. Many attempts have been made to study the structural, electrical, dielectric and magnetic properties of cobalt ferrite in bulk as well as nano-size form [5,6]. In the literature, no systematic investigation of the structural, electrical, dielectric and magnetic properties of aluminum substituted cobalt ferrite is reported. The substitution of non-magnetic Al^{3+} ions in $CoFe_2O_4$ in place of Fe^{3+} ions may lead to magnetic dilution of the system.

2. Experimental technique:

AR grade cobalt nitrate ($Co(NO_3)_2 \cdot 6H_2O$), ferric nitrate ($Fe(NO_3)_3 \cdot 9H_2O$), citric acid ($C_6H_8O_7$), aluminum nitrate ($Al(NO_3)_3 \cdot 9H_2O$), ammonium hydroxide solution (NH_4OH) were used to prepare the aluminum doped cobalt ferrite ($CoAl_xFe_{2-x}O_4$) nanoparticles by sol-gel auto combustion technique. In this chemical process Citric acid was used as a Fuel [7]. An aqueous solution of cobalt nitrate, aluminum nitrates and ferric nitrate were prepared first in stoichiometric proportion and then these solutions were mixed together and stirred for about 1 h. Then citric acid solution was added in the mixed solutions of metal nitrates. These mixed solutions were stirred until the homogeneous solution is obtained simultaneously ammonium

hydroxide solution was added drop by drop to obtain pH of 7. The mixed solution was simultaneously heated at 80 °C for 3 to 4 h to form sol. The transparent sol was further heated to form brown gel. Further increase in a temperature results into combustion of the gel and fine powder of cobalt ferrite nanoparticle was obtained. The powder was dried and annealed at 700 °C for 5h and the same powder was used for further structural, morphological and magnetic characterization.

3. RESULTS AND DISCUSSION

3.1 Structural aspects

3.1.1 X-ray diffraction analysis

Fig.1 shows the X-ray diffraction (XRD) patterns of $\text{CoAl}_x\text{Fe}_{2-x}\text{O}_4$ (where $x= 0.0, 0.2, 0.4, 0.6$) spinel ferrite system. The XRD patterns exhibits single phase cubic spinel structure and exclude the presence of any secondary phase.

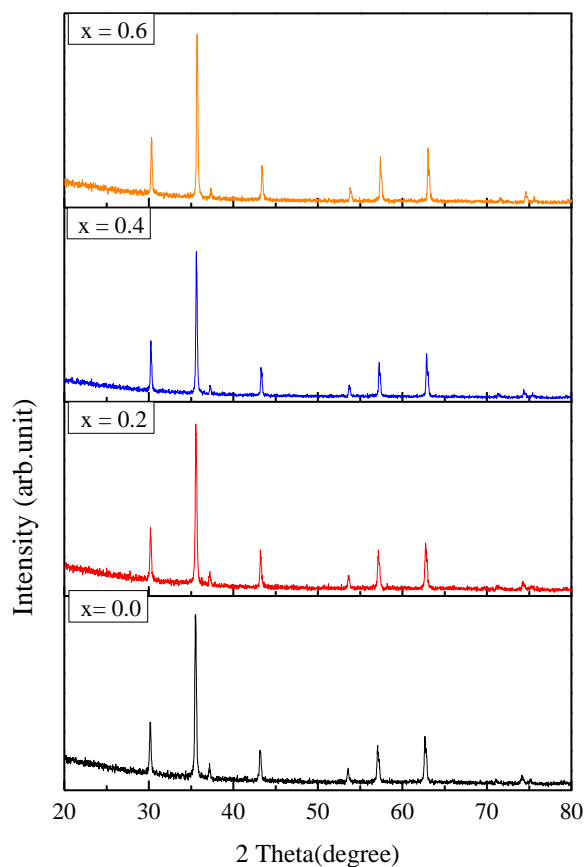


Fig.1. X-ray diffraction pattern of $\text{CoAl}_x\text{Fe}_{2-x}\text{O}_4$ samples

All the reflections which are observed in XRD pattern are slightly broader and less intense which indicate the nanocrystalline nature of the samples. Using the XRD data, it is observed that due to the concentration of non-magnetic Al^{3+} ions in place of Fe^{3+} ions the Bragg's angle shifts towards higher angle and thereby interplanar spacing 'd' values decreases. The lattice constant is found to decrease with increase in aluminum concentration x. The variations in lattice constant as a function of aluminum concentration x can be understood on the basis of the ionic radius of the substituted cations. Since the ionic radius of Al^{3+} ions (0.52\AA) is less than that of Fe^{3+} ions (0.67\AA), the substitution is expected to decrease the lattice constant with increase in aluminum content x [8]. The values of lattice constant obtained from XRD data for varying aluminum concentration x are given in Table 1. The bulk density of each sample was measured by using mass to volume ratio of each sample in the pellet form. The compositional variation of the bulk density (d_b) is given in Table 1. and it has been observed that bulk density decreases with increase in aluminum substitution x. The decrease in bulk density is attributed to the fact that in $\text{CoAl}_x\text{Fe}_{2-x}\text{O}_4$, the mass decreases with aluminum concentration x. The X-ray density (d_x) obtained by using the following relation. [9]

$$d_x = \frac{8M}{N_A a^3} \quad (1)$$

Where, M is molecular weight of the sample, N_A is Avogadro's number and a^3 volume of the unit cell. The X-ray density decreases with increase in Al^{3+} concentration x. The values of X-ray density are given in Table 1. The percentage porosity (%P) was calculated by using the values of X-ray density and bulk density [9]. The values of porosity are given in Table 1. The porosity of the samples increases with aluminum concentration x. The values of porosity are found to be high due to the substitution of aluminum ions. The substitution of aluminum ion reduces the number of ferric ions. The crystallite size of $\text{CoAl}_x\text{Fe}_{2-x}\text{O}_4$ ferrite nanoparticles using the Lorentzian peak (311) was determined from the XRD data using the relations [9]

$$t = \frac{0.9\lambda}{\beta \cos\theta} \quad (2)$$

Where β is the full width at half maximum and λ wavelength of target material.

The values are given in Table 1 and it is observed that the average crystallite size varies between 56 to 32 nm range.

Table. 1

Variation of lattice constant a (\AA), Unit cell volume a^3 (\AA^3) X-ray density d_x (gm/cm^3), bulk density (d_b) (gm/cm^3), porosity (P), Crystallite size (t) of $\text{CoAl}_x\text{Fe}_{2-x}\text{O}_4$ samples.

x	a (\AA)	a^3 (\AA^3)	d_x (gm/cm^3)	d_b (gm/cm^3)	P (%)	t (nm)
0.0	8.3846	589.4501	4.6573	5.145	9.48	56
0.2	8.3746	587.3436	4.5119	5.0276	10.26	47
0.4	8.3592	584.1093	4.3946	4.987	11.88	39
0.6	8.3405	580.198	4.2683	4.980	14.29	32

3.2 Magnetic analysis

The hysteresis plots of $\text{CoAl}_x\text{Fe}_{2-x}\text{O}_4$ system are shown in Fig. 2. The hysteresis plots help us to understand the magnetic response of material and provide the useful information about the magnetic parameters such as saturation magnetization (M_S), Coercivity (H_C) and remanence magnetization (M_r). The magnetic parameters were obtained using hysteresis curve and the values are given in Table 2. The saturation magnetization (M_S) decreases with aluminum concentration x . The decrease in saturation magnetization is related to the magnetic moment of the constituent ions. The decrease in M_S values may be due to the replacement of magnetic Fe^{3+} ($5 \mu_B$) ions by nonmagnetic Al^{3+} ($0 \mu_B$) ions and because of this fact that A-B super-exchange interaction decreases, leading to collapse of magnetic co-linearity of the lattice [9].

The remanence magnetization (M_r) of all the samples under investigation was obtained from M-H plots and the values are presented in Table 2. Overall, the remanence magnetization decreases as aluminum concentration x increases. The remanence magnetization values obtained in the present case proves that the prepared samples are of nanocrystalline nature.

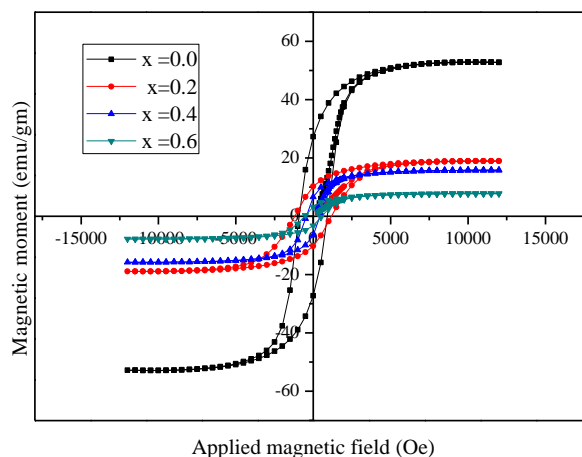


Fig.2. Hysteresis plots of $\text{CoAl}_x\text{Fe}_{2-x}\text{O}_4$ samples.

The plots of magnetic moment versus applied magnetic field provides the useful information regarding the domain state of the samples from the ratio of remanence magnetization to saturation magnetization i.e. M_r/M_s . The values of M_r/M_s of the present samples obtained from M-H plots are given in Table 2. Using M-H plots the Coercivity of all the samples was obtained and the values are presented in Table 2. Our results of the magnetic properties of aluminium substituted cobalt ferrite are in good agreement with the literature reports [10].

Table. 2

Saturation magnetization (M_s), Remanence magnetization (M_r), Remanence ratio (M_r/M_s) and Coercivity (H_c) of $\text{CoAl}_x\text{Fe}_{2-x}\text{O}_4$ system.

x	M_s (emu/gm)	M_r (emu/gm)	(M_r/M_s)	H_c (Oe)
0.0	52.887	27.268	0.51559	910.22
0.2	18.941	10.24	0.540626	1189.0
0.4	15.773	6.5506	0.415305	439.7
0.6	7.7936	3.2302	0.414468	556.58

Conclusions:

The nanocrystalline aluminum substituted cobalt ferrite has been successfully prepared by sol-gel auto-combustion technique. The X-ray diffraction analysis of the samples revealed that the prepared samples possess single phase cubic spinel structure. The lattice parameter obtained from XRD data decreases with increase in aluminum content x . The crystalline size decreases with increase in aluminum content x . The porosity obtained from the values of X-ray density and bulk density increases with increase in aluminum content x . The saturation magnetization (M_s) decreases with increase in aluminum content x . Thus doping of Al^{3+} in cobalt ferrite influences the structural and magnetic properties.

Acknowledgement:

Authors are thankful to Savitribai Phule Pune University, Pune for providing characterization facility. The authors are also thankful to Indian institute of technology, Mumbai for providing characterization facility.

References:

- [1] D.K. Kim, Y. Zhang, W. Voit, K.V. Rao, M. Mohammed, J. Magn. Magn. Mater. 225 (2001) 30.
- [2] M. R. Barati, J Sol-Gel Sci Technol 52 (2009) 171.
- [3] A.T.Raghavendar, Damir Pajic, Kreso Zadro, Tomislav Milekovic, P. Vekateshwar Rao, K.M. Jadhav, D. Ravinder, J. Magn. Magn. Mater. 3 (2007) 204.
- [4] S.E. shirsath, S.M patange, R. Kadam, M. Mane K. Jadhav, J. Mol. Struct. 1024(2012)77
- [5] D.R Mane, U.N Devatwal, K.M Jadhav, Materials Letters 44 (2000)91
- [6] M.Kurian, S.Thankachan,D.Nair,E. Aswathy, Babu Aswathy, A. Thomas, B. Krishna K. T, J. Advanced Ceramics 4(3) (2015) 199-205.
- [7] Vinod N. Dhage, M.L. Mane, M.K. Babrekar, C.M. Kale, K.M. Jadhav, J. Alloys. Compd. 509 (2011) 4394.
- [8] S. P Waghmare, D. M. Borikar, K.G. Rewatkar, Materials today: Proceedings 4(11)(2017) 11866- 11872
- [9] P.S Aghav, Vinod N. Dhage, M.L. mane, D.R. Shengule, R.G. Dorik, K.M. Jadhav, Physica B 406 (2011) 4350-4354.
- [10] Sonal Singhal, S.K Barthwal, kailash Chandra, J. magn. Magn. Mater. 306 (2006) 233.